

# Developing Chitosan Nano particles for the Regulated Administration of Oxytocin: A Physicochemical Study

Dr Mohamed Mutahar RK<sup>1</sup>, Dr. M. Sharath Chandra Goud<sup>2</sup>, Mrs. Koppula Ramya Sree<sup>3</sup>

**ABSTRACT:** This study aimed to characterize and evaluate chitosan nanoparticles (CSNPs) as a carrier system for the hormone, oxytocin. Ionotropic gelation was the technique used to synthesize the CSNPs. Scanning electron microscopy (SEM) and transmission electron microscopy (TEM) showed narrow particle size distribution of 30-50 nm and spherical particle shape. Differential scanning calorimetry (DSC), X-ray powder diffraction (XRD), thermal gravimetric / differential thermal analysis (TGA / DTA) and Fourier Transform Infrared Spectroscopy (FTIR) were used to evaluate possible drug-polymer interactions. Data obtained from X-ray diffraction O-CSNP matrix. Differential scanning calorimetry (DSC) exhibited further evidence of drug-polymer interaction through observed endothermic shifts. Fourier-transform-infrared (FT-IR) spectra obtained confirmed the presence of oxytocin within the CSNP matrix as well as further proof of the intermolecular interactions existing between oxytocin and chitosan. Loading and release profiles of the O-CSNPs were conducted using LC/MS. The effect of nanoparticle size and oxytocin concentration was shown to affect drug loading capabilities and the release behaviour of the O-CSNPs under physiological conditions. *In vitro* release studies were also performed on the O-CSNPs, which exhibited an initial burst effect followed by first-order rate kinetics of oxytocin release from the system. In this work, CSNPs are presented as a potential carrier system for the extended release of oxytocin, thereby improving the efficacy of the hormone in the treatment of neurological disorders.

**Keywords:** Oxytocin, Ionotropic gelation Chitosan, Nanoparticles Tripolyphosphate, Drug delivery

## INTRODUCTION:

The inherent biocompatibility, biodegradability, and non-toxic qualities of the biopolymer chitosan have garnered substantial interest for drug delivery systems using this material. 1. One of the most abundant biopolymers found in nature, chitosan is sourced from crustaceans' exoskeletons, yeast, and the fungal walls of algae. Chitosan comprises repeating units of  $\beta$ -(1-4)-linked D-glucosamine (a deacetylated unit) and N-acetyl-D-glucosamine (an acetylated unit), which are derived from chitin. 3. One distinctive property of chitosan is its ability to cling to

mucosal surfaces and temporarily loosen the tight connection between epithelial cells. 4. The remarkable physicochemical and biological characteristics of chitosan nanoparticles make them promising drug delivery platforms for hydrophilic compounds. 5 to 7. Due to its ability to decrease medication administration frequency while simultaneously minimizing adverse effects and prolonging a medicine's effectiveness, controlled delivery of bioactive compounds has been the subject of a great deal of research compared to standard dosing approaches (8-10).

Professor<sup>1</sup>, Associate professor<sup>2</sup>, Assistant professor<sup>3</sup>  
Department of Pharmaceutics,  
Global College of Pharmacy, Hyderabad. Chilkur (V), Moinabad (M), Telangana- 501504.

Because nanotechnologies may increase the therapeutic index of almost any medicine and open up new non-invasive delivery options including the oral, nasal, and ocular routes of administration, nanoparticles are attracting a lot of interest. Furthermore, nanoparticles have many benefits as medication delivery systems, such as excellent stability, high transport capacity, ease of incorporation into hydrophilic and hydrophobic substances, and the ability to be administered via a variety of methods, including inhalation and oral ingestion. The regulated and sustained release of drugs from the matrix 15 is another potential use of nanoparticle design.

For their possible use in the delivery of antibiotics, peptides, genes, proteins, and anti-cancer medicines, chitosan nanoparticles (CSNPs) have been the subject of extensive study (16–17). Multiple techniques have been developed over the years for synthesizing CSNPs, including ionotropic gelation, microemulsion, emulsification solvent diffusion, and polyelectrolyte complex 18 -

20. These procedures provide gentle and easy preparation methods that do not include organic solvents or strong shear forces. The use of ionotropic gelation to manufacture CSNPs was first documented by Calvo et al., 21 and has since been the subject of much research and development (22, 23). By using ionotropic

The gelation process involves the electrostatic interaction between the positively charged amino groups on chitosan and the negatively charged counterions, leading to the spontaneous production of nanoparticles.

The hypothalamic hormone oxytocin has shown promise in the treatment of autism and a number of neurological conditions, including major depressive disorder and bipolar disorder.

Twenty-four. Oxytocin plays an essential role in many social behaviors across many species. These include trust, fear regulation, face recognition, and pair bonding. Researchers have found trace amounts of oxytocin in the plasma of people suffering from neurological diseases. Current therapeutic uses of oxytocin are limited by frequent dosages and in vivo stability 28, despite the fact that intranasal administration of the hormone has relieved several symptoms associated with these illnesses 26–27. As shown in Figure 1, the nine-amino acid neuropeptide oxytocin takes on the structure postulated by Urey and Walter (29). There has been little investigation into the use of nanoparticles for the regulated administration of oxytocin so far. So, to improve the effectiveness of oxytocin therapy, we offer CSNPs as a possible carrier system for the prolonged release of the hormone.

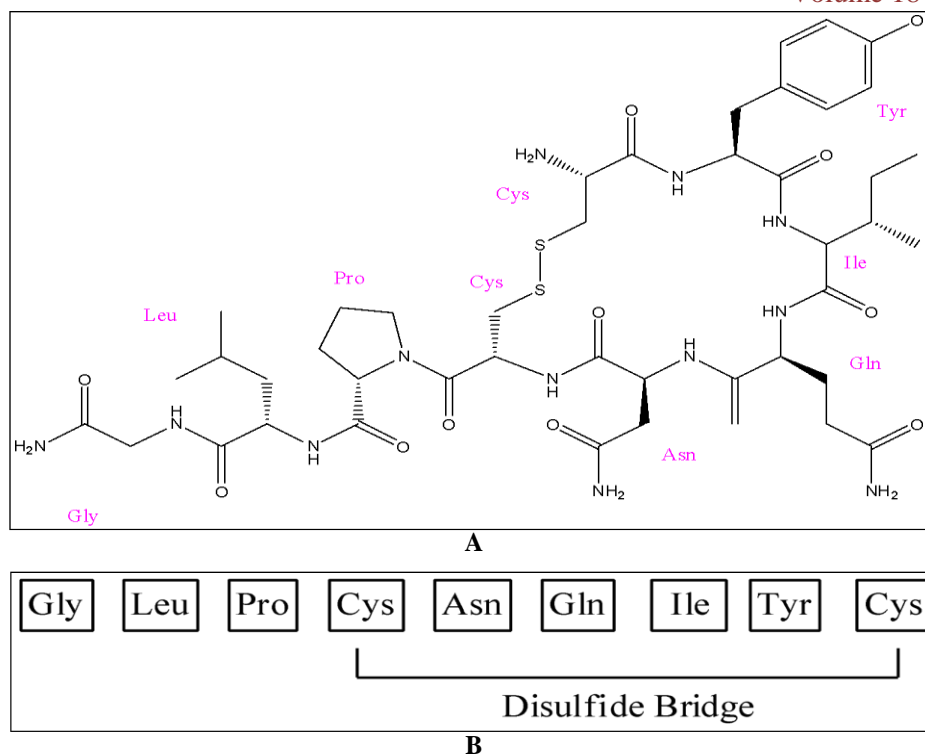


**FIG. 1: CHEMICAL STRUCTURE OF OXYTOCIN (A) IN AQUEOUS SOLUTION (B) AMINO ACID SEQUENCE**

## MATERIALS AND METHODS:

Chitosan (medium molecular weight) and oxytocin were bought from Sigma-Aldrich for the preparation of oxytocin-loaded chitosan nanoparticles. The supplier, Fisher, supplied the pentasodium tripolyphosphate (TPP). No further purification was performed on any of the other components or reagents; they were all of analytical grade.

Rather et al. (30) previously detailed a conventional approach for producing chitosan nanoparticles (CSNPs) by ionotropic gelation of chitosan with TPP. To create a 0.005% (w/v) chitosan solution with a pH of  $5.5 \pm 0.1$ , 25 mg of chitosan was dissolved in 500 mL of 20% acetic acid. In a 1:1 ratio, a 0.025% TPP aqueous solution (pH  $5.4 \pm 0.1$ ) was mixed with a chitosan solution and left to stir at room temperature for 15 minutes. A final concentration of 0.12 mg/ml was achieved by mixing a determined amount (60 mg) of oxytocin into the chitosan solution after stirring it for 2 hours. The nanoparticles were lyophilized after their spontaneous formation to facilitate further analysis.

**Size and Shape of Particles:** The oxytocin-loaded CSNPs were analyzed for size and shape using a Hitachi 4700 SEM and a Zeiss Libra 120 TEM with a Gatan Ultra scan 1000 2k x 2k CCD camera. Prior to scanning electron microscopy (SEM) analysis, samples were double-sided adhesive taped onto aluminum stubs and sputter-coated with a thin coating of gold in a vacuum. Before loading the carbon-coated copper grid with aqueous particle dispersions for transmission electron microscopy (TEM) investigation, the grid was allowed to air-dry at room temperature.

Thermo Scientific's Fourier transform infrared spectrophotometer (FT-IR, Nicolet 6700) with a reflectance ATR stage was used to acquire infrared spectra for the purpose of physicochemical characterization. From 400 to 4000  $\text{cm}^{-1}$ , the samples were scanned with a 4  $\text{cm}^{-1}$  resolution. The crystalline nature of the encapsulated system was investigated by X-ray diffraction measurements. We used a Panalytical powder X-ray diffraction machine to compare the molecular structures of oxytocin and chitosan while they were at room temperature.

Utilizing Cu K $\alpha$  radiation within the angle  $2\theta$  range of 5 - 40 degrees, the X'Pert Siemens D5005 X-ray diffractometer is used. A Perkin-Elmer Pyris Diamond Thermo-gravimetric / Differential Thermal Analyzer was used for the thermostability investigations. Using a heating rate of 5 °C/min throughout a temperature range of 100 °C to 425 °C, thermograms were acquired from 5–10 mg samples.

**Efficient Loading:** We determined the loading efficiency of the CSNP matrix by first measuring the concentration of oxytocin in the centrifugation supernatant, and then using the following formula to the measured amounts.

The linear equation for LE (%) is the product of the total oxytocin used (in IU/mL) and the free oxytocin in the supernatant (in IU/mL) divided by 100.

A Bruker ESQUIRE 3000 LC-MS system was used to quantify oxytocin in the supernatant. At a concentration of 2 micrograms per IU, oxytocin is a potent peptide. The therapeutic values of therapy (18–24 IUs/dose) were used to determine the oxytocin concentration range.

We used LC/MS Table 1 to find out how much oxytocin was in the chitosan nanoparticle. The linearity of the analyte's response proportionate to concentration within defined ranges was determined using an external technique of calibration. Within the concentration range of 9.98–159.6 mg/ml, the standard curve exhibited a linear relationship with 5–80 IUs.

**TABLE 1: LC-MS PARAMETERS FOR LOADING AND RELEASE STUDIES**

Parameters	Values
MS Parameters	
Source	Electrospray Ionization (ESI)
Capillary (kV)	4.5
End Plate Offset (kV)	0.5
Nebulizer (psi)	7.3
Dry Gas (l/min)	4.0
Dry Temperature (°C)	180
Polarity	Positive
ICC	Ultrascan
Target	200,000
Max. Accu. Time (ms)	200
Scan (m/z)	100-2800
Averages	5
LC Parameters	
Pump (mL/min)	0.2
Pressure (psi)	1800
Injection volume (ul)	5

**RESULTS:** A proposed schematic for the binding of oxytocin to chitosan in the preparation of O- CSNPs is illustrated in **Fig. 2**, where oxytocin was incorporated into chitosan solution before crosslinking with tripolyphosphate (TPP) under acidic conditions. In solution, the following intramolecular hydrogen bonds are formed: C=O from Cys → N-H from Gly, Peptide C=O from Asn → N-H Tyr, and side chain C=O from Asn → N-

H Leu<sup>29</sup>, which are unavailable for hydrogen bonding. In this work, it is proposed that the two available amino acids of Gln and Cys from oxytocin are available for intermolecular hydrogen bonding through the hydroxyl groups on the chitosan backbone. This interaction was studied using FTIR, XRD, and TGA/DTA. Morphology and particle size distribution were examined by SEM and TEM.

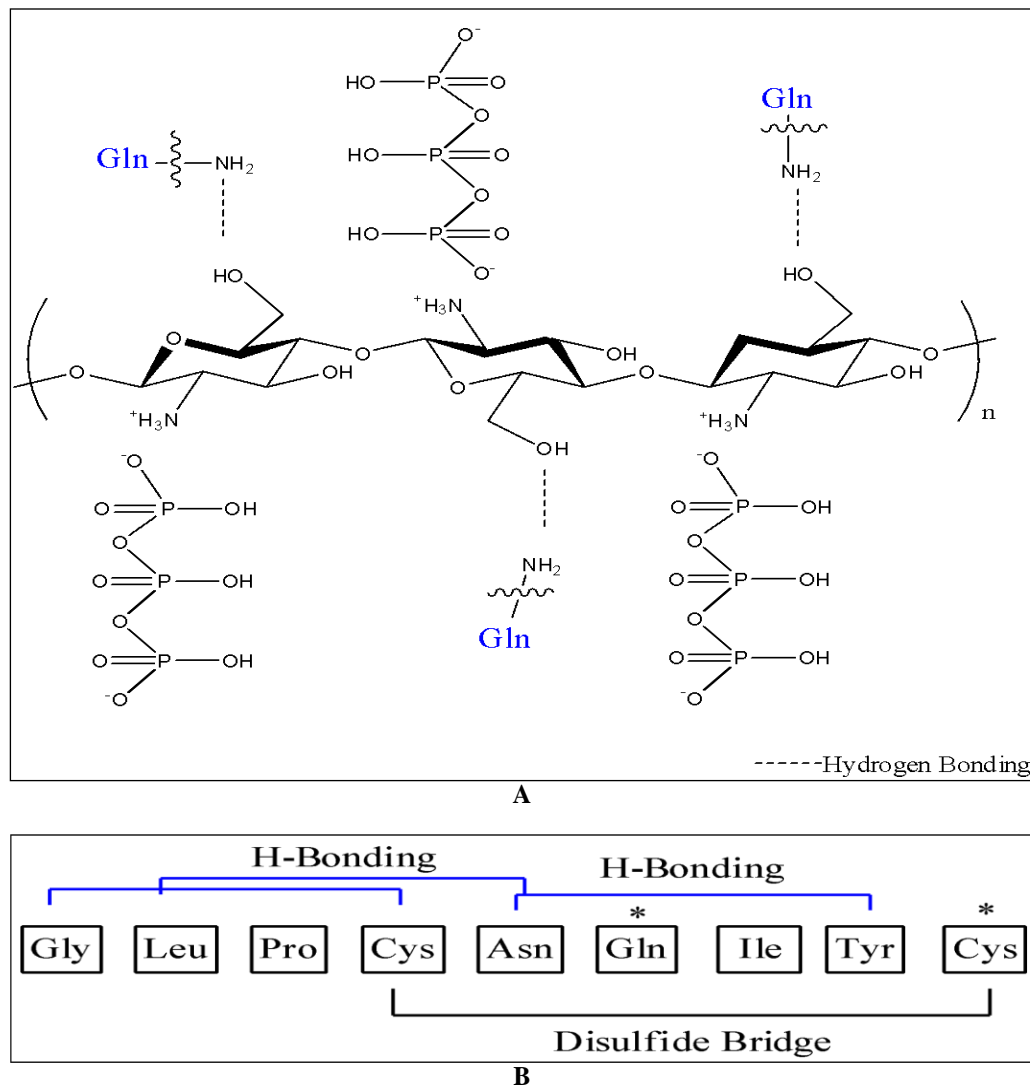
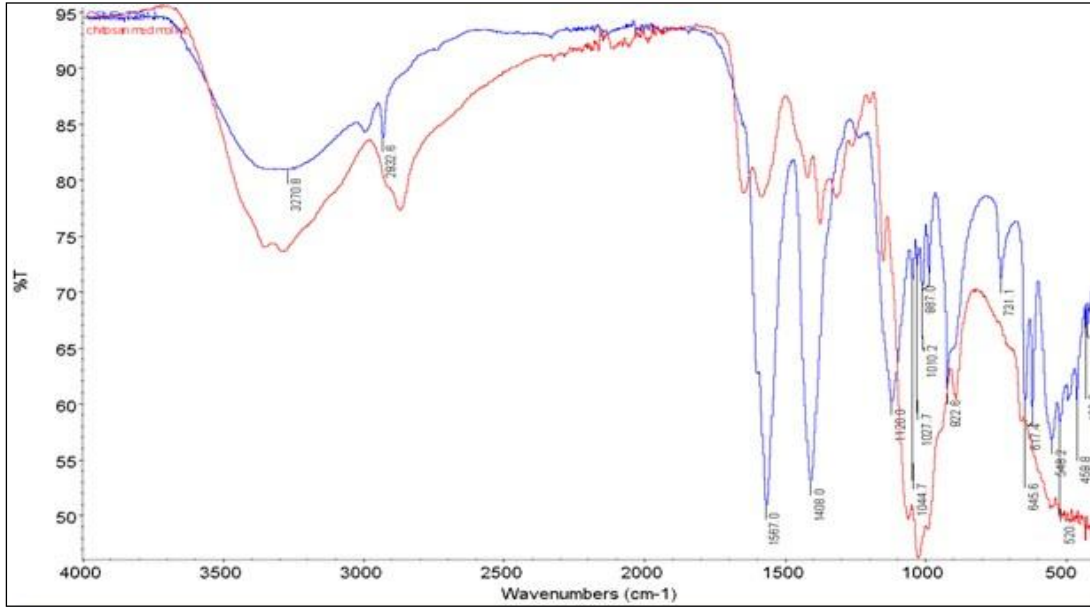


**FIG. 2: PROPOSED SCHEMATIC OF OXYTOCIN-CHITOSAN INTERMOLECULAR INTERACTION (A) HYDROGEN BONDING EXISTING BETWEEN HYDROXYL GROUPS ON CHITOSAN AND GLY ON OXYTOCIN (B) AMINO ACID SEQUENCE DENOTING GLY AND CYS AMINO ACIDS AVAILABLE FOR HYDROGEN BONDING**

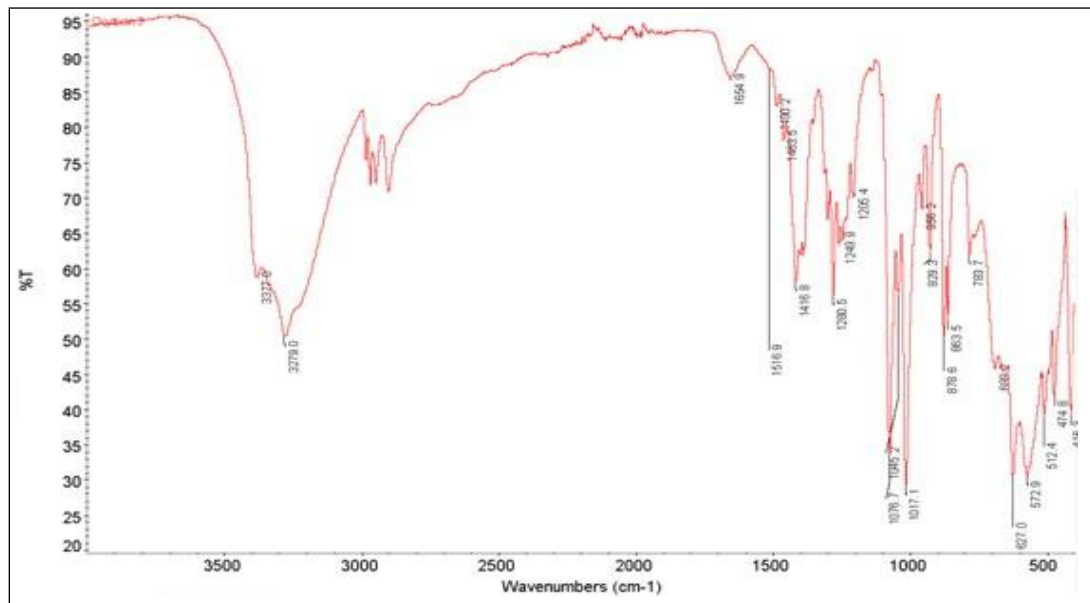
**Physicochemical Characterization:** FTIR spectra in Fig. 3A - C show characteristic peaks of chitosan at  $3429\text{ cm}^{-1}$  for the -OH and -NH<sub>2</sub> group stretching vibrations as reported by Hosseinzadeh *et al.*,<sup>31</sup>. A peak at  $1645\text{ cm}^{-1}$  is due to the carbonyl stretching vibration in amide group (amide I vibration), and the peak at  $1583\text{ cm}^{-1}$  is due to N-H

bending vibrations of the secondary amide. Absorption bands in the region of  $1149\text{ cm}^{-1}$  and  $1031\text{ cm}^{-1}$  are representative of anti-symmetric stretching of the C-O-C bridge and C-O stretching vibrations, which are characteristic of the chitosan saccharide structure as previously reported<sup>31</sup>. Upon formation of chitosan nanoparticles (CSNPs)

crosslinked with TPP, a small band at  $1215\text{ cm}^{-1}$  is observed due to the stretching vibrations of P=O as previously reported by Gierszewska-Drużyńska<sup>32</sup>. The peak shift from  $1583\text{ cm}^{-1}$  to  $1567\text{ cm}^{-1}$  represents the -NH<sub>2</sub> bending vibration, which was attributed to the linkage between tripolyphosphoric and ammonium group of NH<sup>3+</sup> of chitosan. The FTIR spectra of oxytocin exhibits characteristic peaks of amide II stretching, which ranges from  $1520$  to  $1580\text{ cm}^{-1}$  as a result of N-H and N-C deformations of the backbone peptide groups. The amide I region is observed at  $1620$  to  $1700\text{ cm}^{-1}$  caused by the carbonyl stretching of the backbone peptide groups. A smaller absorbance at  $1510\text{ cm}^{-1}$  caused by the tyrosine side chain O-H deformation is also observed. The presence of the oxytocin disulfide bridge (C-S-S-C) is evident by the bands occurring from  $570 - 705\text{ cm}^{-1}$ <sup>133</sup>. FTIR spectra of oxytocin loaded chitosan nanoparticles (O-CSNPs) confirm drug-polymer interaction through the observation of increased hydrogen bonding between the hydroxyl groups on chitosan and available amino acid groups of oxytocin as evidenced by the broadened OH stretching at  $3400\text{ cm}^{-1}$  and a shift in the -OH deformation stretch from  $887\text{ cm}^{-1}$  to  $922\text{ cm}^{-1}$ . The presence of oxytocin in O-CSNPs was observed in the native disulfide stretch within the  $570 - 705\text{ cm}^{-1}$  range.



A



B

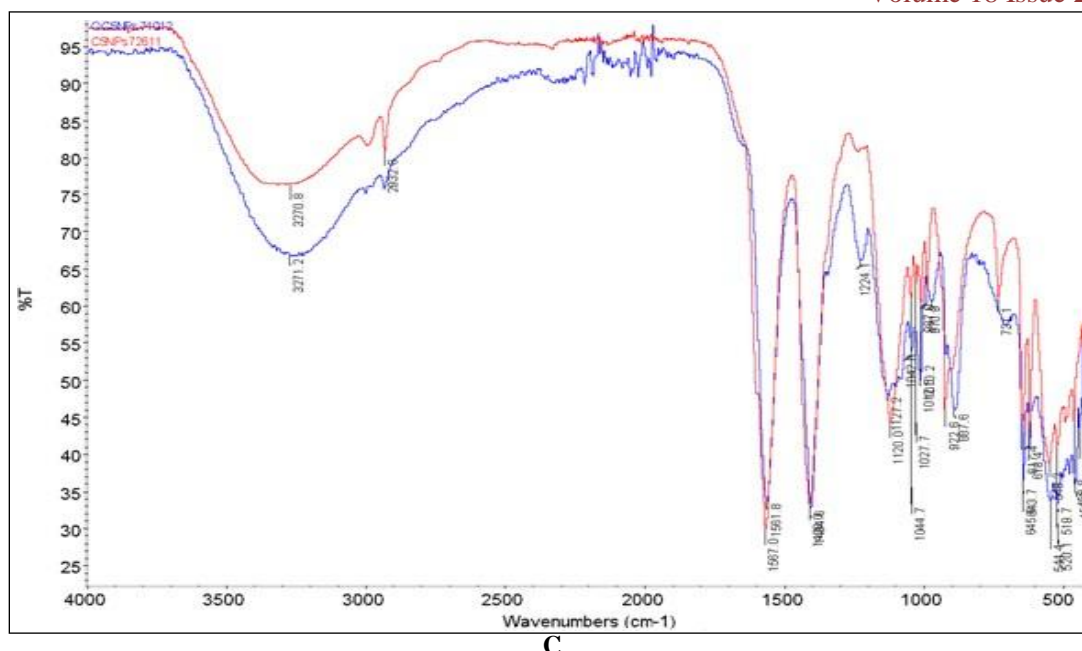


**FIG. 3: FTIR SPECTRA OVERLAY (A) CHITOSAN (RED) AND CSNPs (BLUE) (B) SPECTRA OF OXYTOCIN (C) OVERLAY OF CSNPs (RED) AND O-CSNPs (BLUE)**

Once oxytocin was integrated into the polymeric nanoparticles, its degree of crystallinity and physical condition were examined using X-ray diffraction (XRD). Comparing the XRD patterns of oxytocin, CSNPs, and O-CSNPs showed that the molecular state of oxytocin changed significantly after incorporation into the CSNP matrix. The presence of a wide peak at  $20^\circ$  ( $2\theta$ ) in native chitosan powder indicates that it is mostly an amorphous form of chitosan 32. The inset view of Figure 4 shows that when the CSNPs are crosslinked with TPP, the peak's intensity drops and moves somewhat, suggesting that the CSNPs get a less crystalline structure. According to earlier reports, the disarray in chain alignment and

consequent loss in crystallinity 34 is caused by the crosslinking of TPP counter ions, which disrupts the intermolecular and intramolecular network structure of CS. The diffractogram for oxytocin showed many distinct crystalline peaks at  $22^\circ$ ,  $28^\circ$ ,  $31^\circ$ ,  $33^\circ$ ,  $35^\circ$ , and  $38^\circ$ , according to the  $2\theta$  values. The amorphousness of CSNPs increased after oxytocin loading. The observed reduction in crystallinity was likely caused by alterations in the supramolecular structure of chitosan nanoparticles. These alterations would have resulted from the formation of intermolecular hydrogen bonds between oxytocin and chitosan and the breaking of intramolecular hydrogen bonds within chitosan.

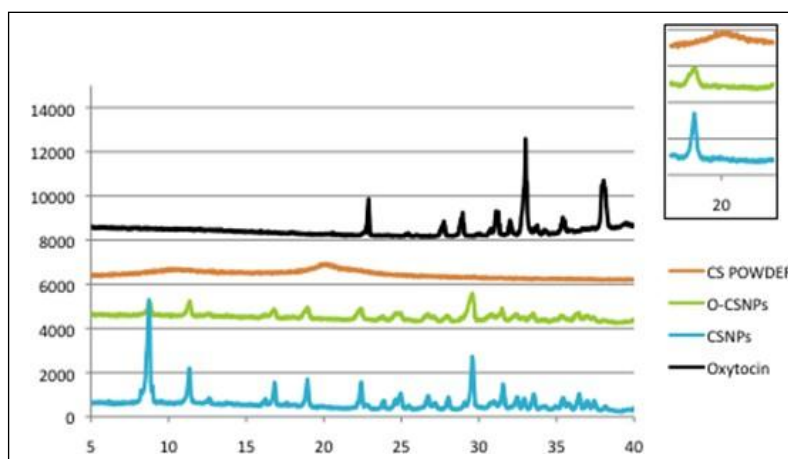


**FIG. 4: XRD OF CS POWDER (ORANGE), CSNPs (BLUE), O-CSNPs (GREEN), AND OXYTOCIN (BLACK)**



Utilizing thermogravimetry and differential thermal analysis (TGA/DTA), the impact of cross-linking and oxytocin loading on the thermal stability of chitosan was investigated. Figure 5 shows that at temperatures below 100 °C, native CS begins to lose water, and around 275 °C, deterioration begins. Crosslinking was shown to reduce the system's thermostability. Similarly, Denuziere et al., 35 found that crosslinking altered the molecular structure of chitosan, which reduced its heat stability. In order to verify the drug-polymer interactions, DTA was performed on CSNPs, oxytocin, and O-CSNPs. An endothermic melting peak at 166.61 °C was shown by the DTA for pure oxytocin. Two distinct features are shown by the DTA of CSNPs.

the endotherms that may be attributed to the dissociation of hydrogen bonds and degradation, which occur at 105.02 and 121.39 °C, respectively, and a degradation temperature of 313.89 °C. As seen in the inset of Figure 5, there is a little shift in the exothermic peak from 235.88 °C to 242.04 °C, and the two endotherms at 105.02 °C and 121.39 °C combine, in contrast to O-CSNPs. These changes show that oxytocin and chitosan are interacting, which is probably because, as shown in Fig. 2, the two amino acid groups that are accessible in oxytocin (Gln and Cys1) form hydrogen bonds with the hydroxyl groups on chitosan. The fact that the oxytocin endothermic peak is no longer present in O-CSNPs indicates that the loaded nanoparticles contain little amounts of free hormone.

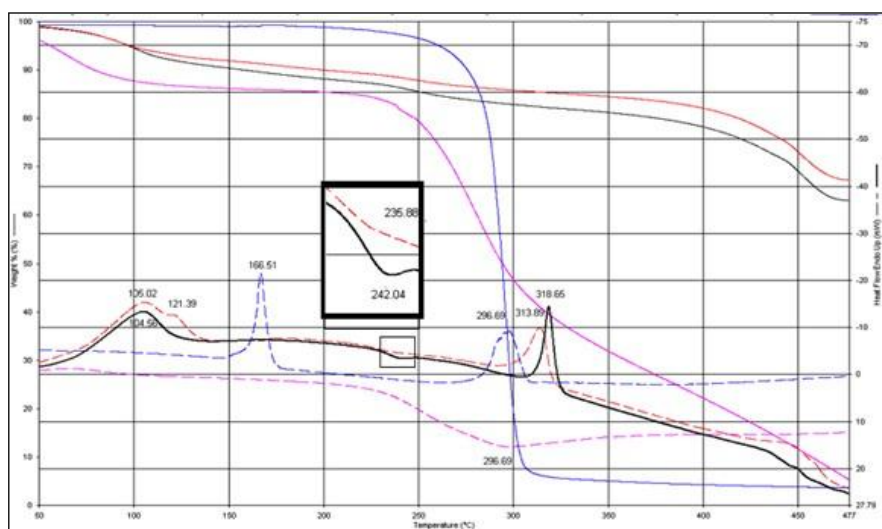


**FIG. 5: TGA / DTA OF CHITOSAN, OXYTOCIN (BLUE), CS POWDER (PINK), CSNPs (RED), AND O-CSNPs (BLACK)**

Scanning electron micrographs of CSNPs are shown in **Fig. 6A - D**. CSNPs were observed to be spherical with an average size of about 30 - 50 nm.

TEM confirmed that CSNPs were spherical with a uniform size distribution **Fig. 7A, B**.

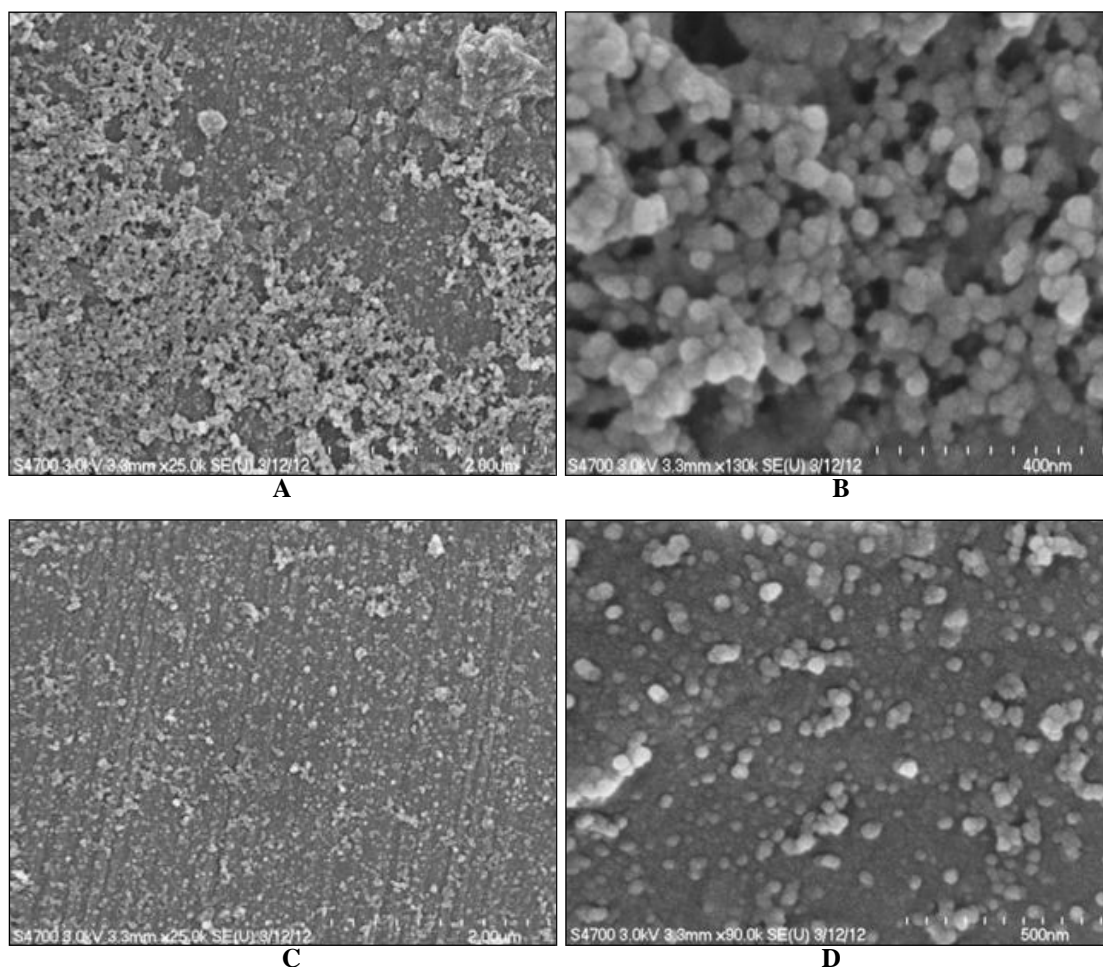


**FIG. 6: SCANNING ELECTRON MICROGRAPHS OF CSNPs A) 40K, B) 150K, C) 40K, D) 150K MAGNIFICATIONS**

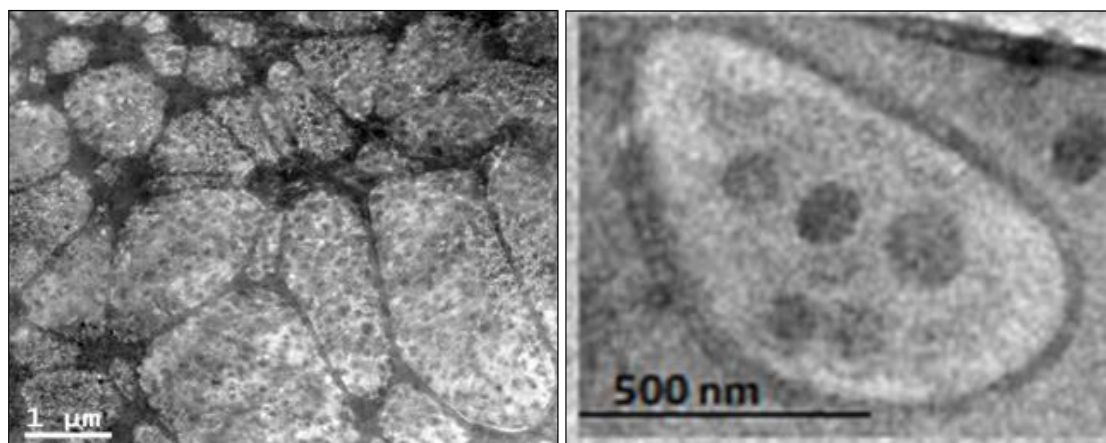


**FIG. 7: TRANSMISSION ELECTRON MICROGRAPHS OF CSNPs 40 K MAGNIFICATION (LEFT) AND 150 K MAGNIFICATION (RIGHT)**

**Loading:** CSNPs were loaded with oxytocin at various concentrations (10 - 30 IU/ml) to find the optimal loading efficiency. This range was selected based on the therapeutic range of oxytocin used in biomedical applications. The loading efficiency of the CSNPs is inversely related to oxytocin concentration up to about 25 IU/ml **Fig. 8**, which was determined to be the optimal loading concentration.

The effect of particle size on loading efficiency was also observed **Fig. 9**, and it was determined that larger particles have fewer available sites for oxytocin binding, whereas smaller particles have more sites available for oxytocin-chitosan interaction due to a higher surface area. When the nanoparticle size was optimized to 50 nm, the loading capacity was shown to increase to 90% **Fig. 9**.

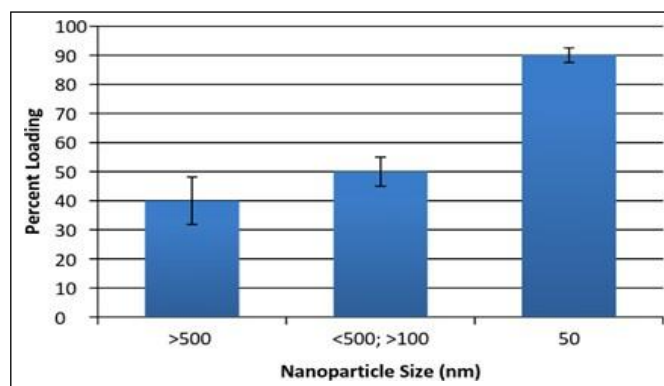
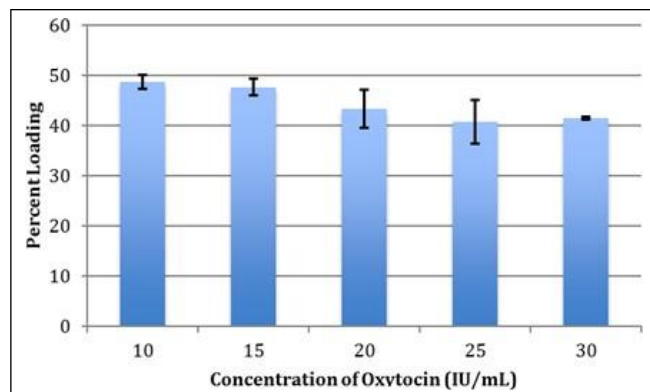


**FIG. 8: LOADING EFFICIENCY OF CSNPs**

**FIG. 9: THE EFFECT OF PARTICLE SIZE ON LOADING EFFICIENCY (OXYTOCIN CONCENTRATION 25 IU/mL)**



**Release Studies:** Oxytocin-loaded CSNPs (O- CSNPs) were centrifuged, and the supernatant was separated by LC and identified by EI-MS at various times over 24 - 72 hr. **Table 2** shows the EI mass spectra data of oxytocin released into the supernatant from single - crosslinked CSNPs at different intervals. The UV quantifies the concentration at which oxytocin was released into

**TABLE 2: RELEASE PROFILE OF O-CSNPs**

the supernatant in tandem with MS, which confirmed the target analyte. No release of oxytocin is observed (A, B) until after 1 hour when a ‘burst’ (32.3%) effect of oxytocin occurs as shown in Table 2. This amount (32.3 - 38.5%) is sustained (C, D, E) for up to 24 hours, after which elevated levels of oxytocin is observed due to the erosion of the CSNP matrix.

	Time (hours)	Target Analyte	Extracted Ion Peak Mass (m/z)	Retention Time (min)	Mean Absorbance (mAU)	% Release	Standard Deviation
A	0	Oxytocin	1007.5	0	0	0	0
B	0.5	Oxytocin	1007.5	0	0	0	0
C	1	Oxytocin	1007.5	7.4	19.3	32.3	3.1
D	1.5	Oxytocin	1007.5	7.4	3.3	37.8	2.6
E	24	Oxytocin	1007.5	7.4	0.4	38.5	1.5
NS	48	Oxytocin	1007.5	7.4	2.9	43.3	5.8
NS	72	Oxytocin	1007.5	7.4	25.2	85.3	5.5

\*NS- Not shown due to degradation of CSNP matrix. LC-UV and MS are run in tandem

***In vitro* Release Profile of Oxytocin from CSNPs using LC-MS:** *In vitro* dissolution testing using phosphate buffered saline is an essential well- characterized method for screening drug formulations before moving onto *in vivo* studies that evaluate the efficacy of the delivery system. The release profile of oxytocin-loaded CSNPs (O- CSNPs) was investigated under physiological conditions using phosphate buffered saline (pH 7) over 72 hours to evaluate the rate at which oxytocin was released from the chitosan nanoparticles and to quantify the number of days the hormone remained stable before degradation occurred. The hormone release from TPP-crosslinked CSNPs (O-CSNPs) showed 40% of the hormone was released over a 24 hour period.

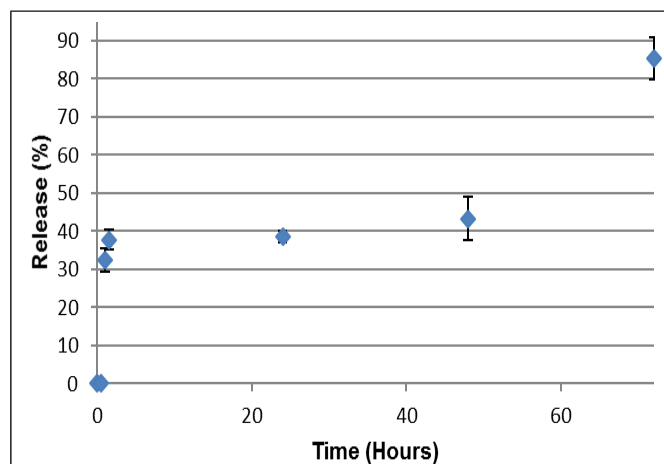


**FIG. 10: THE RELEASE PROFILE OF OXYTOCIN FROM CSNPs SINGLE - CROSSLINKED WITH TPP OVER 72 HOURS**

The initial rapid drug release from the single- crosslinked nanoparticles was due to the release of oxytocin from the surface of the nanoparticle. A similar release profile was reported by Elgadir *et al.*,<sup>13</sup> for the release of silver sulfadiazine from a bilayer chitosan dressing that exhibited a burst release on the day one and then abated to a much slower release. Nallamuthu *et al.*, also reported the sustainable release of chlorogenic acid from crosslinked chitosan nanoparticle<sup>36</sup>.

## CONCLUSION:

This study demonstrates a rapid, mild method for preparing oxytocin - loaded chitosan nanoparticles. Morphology and particle size using SEM and TEM show nanospherical particles ranging from 30 - 50 nm in size. XRD patterns showed a molecular dispersion of oxytocin within the CSNP matrix and an observed decrease in crystallinity upon crosslinking and loading of oxytocin due to the disruption in the intramolecular / intermolecular chitosan network. FTIR and

TGA / DTA confirmed oxytocin - chitosan intermolecular interaction. Results support the hypothesis that chitosan nanoparticles could be a valuable tool in the controlled-release of hormones for therapeutic applications.

The loading efficiency of oxytocin onto the CSNPs was studied as an effect of particle size and results showed that the loading capacity of the nanoparticles is inversely related to the size. A maximum loading capacity of 90% was attained upon particle size reduction to 50 nm.

Release studies were performed and involved the following 3-stage release profile: burst, sustained, erosion. The O-CSNPs showed an initial burst effect within the initial 24hr period due to the release of surface adsorbed oxytocin, followed by a sustained period of release of oxytocin from the pores and channels of the nanoparticles, and final erosion of the chitosan matrix at 72 hours.

With the development of a CSNP matrix exploiting the intermolecular hydrogen bonding between the amine groups of chitosan and available amino acids of oxytocin, the effects of oxytocin are sustained longer under physiological conditions. By optimizing of the intermolecular bonding of chitosan nanoparticles, we have enhanced oxytocin stability under physiological conditions for a prolonged period. This enhanced stability, in turn, will increase the length of time chitosan is adsorbed to the mucosal lining of the nasal cavity, which will increase the bioavailability and absorption of oxytocin.

## REFERENCES:

1. The use of chitosan-based nanoparticles in biomedical applications by Laskar and Rauf. The article "Nanomed Res J 2017; 5(2): 00112" is printed in the journal *Nanomed Research*.
2. Chitosan and its preparation derived from marine sources by Younes and Rinaudo. Structures, characteristics, and use. *Drugs*, March 2015, vol. 13, no. 3, pp. 1133–1174. publishable at doi:10.3390/md13031133
3. Chitosan: A review of its possible uses in medicine and pharmaceuticals (Cheung RCF, Ng TB, Wong JH, & Chan WY). Edited by Laurienzo P. *Journal of Drugs*, March 2015, 13(8), 5156-5186. this article's DOI is 10.3390/md13085156.
4. An investigation of the process by which goblet cell-specific trimethyl chitosan nanoparticles induce cellular absorption and tight junction opening was conducted by Zhang, Jin, Shan, and Huang in a 2004 paper. The citation is from *Mol. Pharm.* 2014, volume 11, issue 5, pages 1520–1532. published online at 10.1021/mp400685v.
5. Bioproduction of chitooligo saccharides: Present and prospective (Jung WJ and Park RD). *Pharmaceuticals*, March 2014, 12, 5328–5356.
6. Walke S, Srivastava G, Nikalje M, Doshi J, Kumar R, Ravetkar S and Doshi P: Antibacterial, antioxidant, and tetanus toxoid entrapment effectiveness of chitosan produced from shrimp shells and examination of its physicochemical and functional characteristics. Article published in 2014 in the *International Journal of Pharmaceutical Science Review and Research*, volume 26, issue 2, pages 215-222.

7. The construction of chitosan microcapsules filled with lactobionics as prospective medication carriers for the liver was carried out by Zhang XZ, Li C, Xue ZY, Cheng HW, Huang FW, Zhuo RX, and Zhang J. *Acta Biomaterialia*, 2011, 7, 4, 1665–1673.
8. A review of chitosan nanoparticles and their uses in medication administration by Najafi, Pazhouhnia, Ahmadi, Berenjani, and Jafarizadeh-Malmiri. Presented in the 2014 edition of *Current Research in Drug Discovery*, volume 1, issue 1, pages 17–25.
9. An Impact of Chitosan Composites and Chitosan Nanoparticle Composites on Different Drug Delivery Systems (Elgadir A, Uddin S, Ferdosh S, Adam A, Khan AJ, and Sarker ZI). The citation is from the *Journal of Food and Drug Analysis*, volume 23, issue 4, inside the pages 619-629 of 2015.
10. "Biocompatibility of chitosan carriers with application in drug delivery" was published by Rodrigues et al. (2010). *Functional Biomaterials*, 2012, 3, 615-641.
11. Poonia N, Kharb R, Lather V and Pandita D: A Versatile oral delivery vehicle: nanostructured lipid carriers. The article may be found in *Future Science OA* 2016; 2(3): FSO135 and the DOI is 10.4155/fsoa-2016-0030.
12. Reviews the possibilities of stimuli-responsive nanogels for targeted treatment medication and active chemical administration (Vicario-de-la-Torre M and Forcada J, 2012). Vol. 3, No. 16, 2017, pp. 1–37.
13. The authors are Patel A, Patel M, Yang X, and Mitra AK. Polymeric nanoparticles have recently emerged as a viable option for the delivery of peptides and proteins drugs. *Journal of Protein and Peptide Science*, 2014, vol. 21, no. 11, pp. 1102-1120.
14. Chapter fourteen: Bhatia S. *Nanotechnology for Drug Delivery*. Academic Press, Apple, 2016.
15. Chen W, Guo D, Sun L, Fan Y, Guo F, Zheng Y, and Chen Y: A research on the sustained release of 5-fluorouracil-loaded chitosan nanoparticles in vitro and in vivo. The citation is from the 2017 issue of the *Asian Journal of Pharmaceutical Sciences*, volume 12, issue 5, pages 418-423.
16. Ding RL, Xie F, Hu Y, Fu SZ, Wu JB, Fan J, He WF, He Y, Yang, LL, Lin S, and Wen QL: Antitumor efficacy of endostatin-loaded chitosan nanoparticles and their preparation using the Lewis lung cancer model. *Medical Delivery*, 2017; 24(1): 300-308. 10.1080/10717544.2016.1247927 is the DOI for the article.
17. A Potential Cancer Therapy: Peptide-Based Treatment (Xiao YF, Jie MM, Li BS, Hu CJ, Xie R, Tang B, and Yang SM, 2017). Article ID 761820 from the *Journal of Immunology Research* in 2015, pages 1-13.18. Rajatha P, Gopinath D, Biswas R, Sabitha M, and Jayakumar R: Chitosan nanoparticles in the pharmacological treatment of inflammatory and infectious disorders (doi:10.1155/2015/761820). *Expert Views on Medication Administration* publication year: 2016; volume: 13, issue: 8; pages 1177–1194. Chitosan nanoparticles—a new development in nanotechnology (Rajalakshmi R, Muzib Y, Aruna U, Vinesha V, Rupangada V, and Krishna Moorthy SB, 2016). Results from the 2014 *International Journal of Drug Delivery*, 6:



204-229.

18. A nanoparticle-based insulin delivery method was developed by Sharma G, Sharma AR, Nam JS, Doss GPC, Lee SS, and Chakrabo C.
19. Efficacious treatment for type 1 diabetes in the future. "Journal of Nanobiotechnology" (Volume 13, Issue 74, 2015).
20. New protein and vaccine carriers using chitosan and chitosan/ethylene oxide-propylene oxide block copolymer nanoparticles, as reported by Calvo, Remuñan-López, Vila-Jato, and Alonso MJ. Article published in *Pharmaceutical Research* in 1997, volume 14, pages 1431–1436.
21. An review of recent achievements in chitosan nanoparticles made by ionotropic gelation: Desai KG, 22. The number of reviews for therapeutic drug carrier systems was 33 in 2016, with pages 107–58.
22. [23] Kouchak M and Azarpanah A: Ion-gelation approach for the preparation and in vitro assessment of chitosan nanoparticles containing diclofenac. The article "Intranasal oxytocin in the treatment of autism spectrum disorders: A review of literature and early safety and efficacy data in youth" was published in the *Jundishapur Journal of Natural Pharmaceutical Products* in 2015 and can be found on page 23082. The authors are Anagnostou, Soorya, Brian, Dupuis, Mankad, Smile, and Jacob. *Journal of Brain Research*, 2014, 1580, 188–198.
23. Twenty-five. Lieberwirth C and Wang Z: Neuropeptide modulation of social bonding. Publication date: 2014; volume: 8; page number: 171. 26. Quadrocki E and Friston K: Interoception, oxytocin, and autism (doi:10.3389/fnins.2014.00171). Paper published in 2014 in the journal *Neuroscience and Biobehavioral Reviews*, volume 47, pages 410–430. Article 27. doi:10.1016/j.neubiorev.2014.09.012.A thorough analysis of oxytocin and its pro-social effects in humans: The Peptide that Binds (K. Macdonald and TM Macdonald). *Psychiatry in Harvard Review* of 2010; 18(1): 1–21. 28. Review of scientific and clinical research results on the function of oxytocin in mental diseases by Cochran, Fallon, Hill, and Frazier JA. Article published in 2013 by the *Harvard Review of Psychiatry*, volume 21, issue 5, pages 219–247. DOI: 10.1097/HRP.0b013 e3182a75b7d.